ORGANIC CHEMISTRY

FRONTIERS

Accepted Manuscript

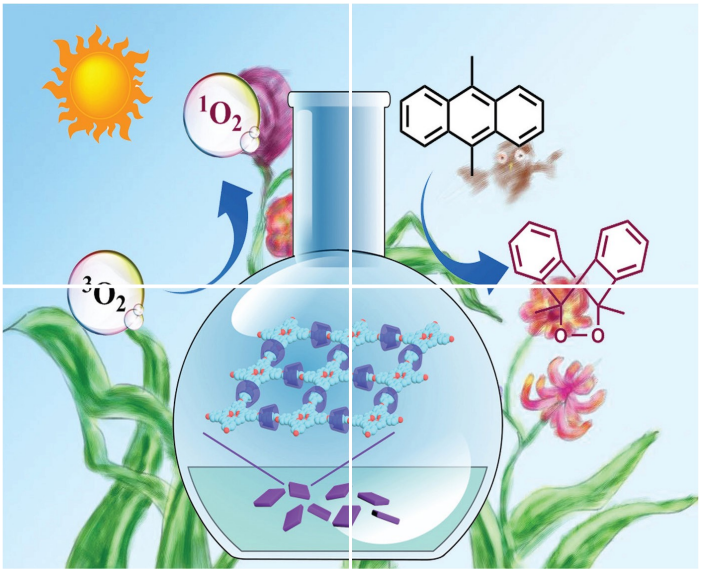

This article can be cited before page numbers have been issued, to do this please use: Y. Gui , X. Li, T. Fu, T. Liang, Z. Li, S. Zhao and Z. Zhang, *Org. Chem. Front.*, 2025, DOI: 10.1039/D5QO00868A.

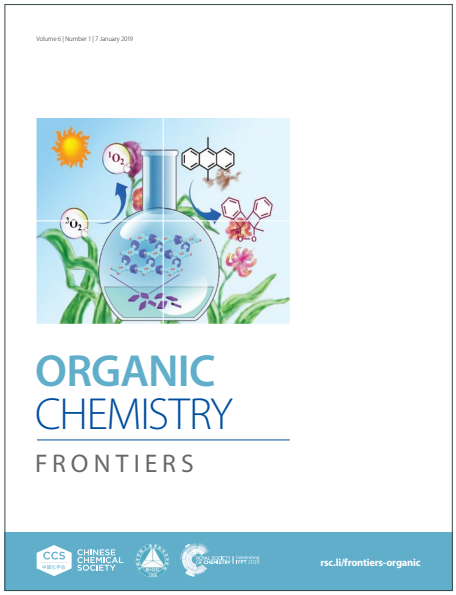

View Article Online
DOI: 10.1039/D5QO00868A

ARTICLE

Ru(II)-Catalyzed Direct Alkynylation of 2-Acylimidazoles with TIPS-Alkynes or TIPS-Bromoalkynes under Air

Received 00th January 20xx,
Accepted 00th January 20xx

DOI: 10.1039/x0xx00000x

Yuting Gui,[‡a] Xingchi Li,[‡a] Ting Fu,[a] Taoyuan Liang,[a] Zequan Li,[b] Shuangliang Zhao*,[a] and Zhuan Zhang*,[a]

The Ru(II)-catalyzed *ortho*-alkynylation of 2-acylimidazoles is reported, demonstrating compatibility with TIPS-protected terminal alkynes or TIPS-protected bromoalkynes as alkynylating reagents. The reaction tolerates a wide range of functional groups, and the resulting alkynylated products can be readily transformed into high-value compounds, presenting promising applications in medicinal chemistry and materials science. This strategy addresses the existing gap by proposing that the alkynylation reaction proceeds through six-membered ruthenacycle intermediates.

Introduction

Imidazole and its derivatives are highly significant due to their crucial roles in medicinal chemistry and materials science.[1] Their remarkable versatility has led to their incorporation into numerous clinically used drugs, including antifungal, antiparasitic, anesthetic, and antihypertensive agents, among others, which exhibit high therapeutic efficacy and market value (Scheme 1a).[2] Furthermore, 2-acylimidazoles serve as pivotal molecular building blocks, enabling the synthesis of a wide array of bioactive compounds.[3] Their adaptability in structural modification underscores their potential as powerful tools in organic synthesis, offering promising avenues for developing novel pharmaceuticals and functional materials.[4]

Alkynes are fundamental building blocks in synthetic chemistry and materials science.[5] While aryl alkynes are commonly synthesized from aryl halides *via* the Sonogashira reaction,[6] a more desirable and attractive approach leverages the abundance of C–H bonds in arenes through transition-metal-catalyzed C–H activation. This strategy has been extensively explored over the past several decades, leading to the development of numerous synthetic methods for constructing complex structures.[7] Transition-metal-catalyzed direct alkynylation of C–H bonds is particularly advantageous, as it enables direct functionalization without the need for preactivation–a key benefit in the late-stage modification of complex molecules. Pioneered by the work of Chatani,[8] Li,[9] Ackermann,[10] Yu,[11] and Krische,[12] direct alkynylation of C–H bonds has been achieved through the exploration of diverse transition-metal catalysts, enabling access to a wide array of molecular architectures (Scheme 1b).

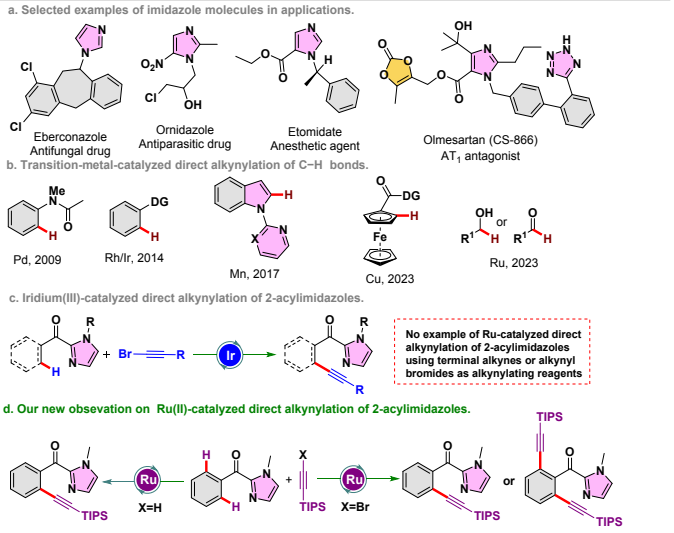

Scheme 1 Previous works and our new observation

Extensive efforts have been devoted to the functionalization of 2-acylimidazoles due to their broad applications. Various transformations, including arylation, alkylation, alkenylation, amidation, esterification, and trichloromethylation, have been explored.[3b, 13] In 2020, Chatani and coworkers reported an Ir-catalyzed alkynylation of 2-acylimidazoles using bromoalkynes, leveraging the imidazole moiety as a directing group through a novel chelation system (Scheme 1c).[14] Despite these advances, Ru-catalyzed direct alkynylation of 2-acylimidazoles remains unexplored. Herein, we disclose a Ru(II)-catalyzed protocol for the direct alkynylation of 2-acylimidazoles with terminal alkynes or alkynyl bromides as versatile alkynylating reagents *via* six-membered ruthenacycle intermediates for the first time. This method features different alkynylating reagents available, high atom economy, excellent functional group tolerance, and the unique advantage of

[a]*Guangxi Key Laboratory of Petrochemical Resource Processing and Process Intensification Technology, School of Chemistry and Chemical Engineering, Guangxi University, Nanning 530004, China;* [b]*School of Resources, Environment and Materials, Guangxi University, Nanning 530004, P. R. China.*
E-mail: szhao@gxu.edu.cn (S. Zhao), zhuan.zhang@gxu.edu.cn (Z. Zhang)
† Electronic supplementary information (ESI) available: Experimental details and NMR spectra for all compounds. CCDC 2417911 (**4sa**). For ESI and crystallographic data in CIF or other electronic format see DOI: 10.1039/x0xx00000x
‡These authors contributed equally to this work.

View Article Online
DOI: 10.1039/D5QO00862A

facile imidazole removal, enabling straightforward conversion to esters under mild conditions (Scheme 1d).

Results and discussion

Table 1 Optimization of the reaction conditions[a]

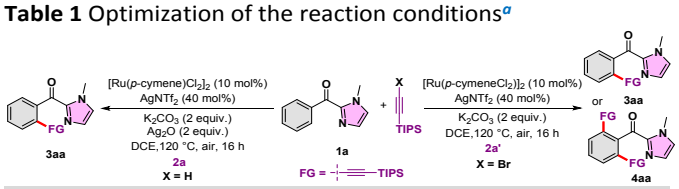

Entry	Variation from "standard conditions"	Yield (%)[b] 3aa/4aa
1	none	73/–
2	CH_3CN instead of DCE	64/–
3	toluene instead of DCE	31/–
4	1,4-dioxane instead of DCE	50/–
5	AgOAc instead of Ag_2O	63/–
6	Ag_2CO_3 instead of Ag_2O	59/–
7	$Cu(OAc)_2$ instead of Ag_2O	n.d/–
8	K_3PO_4 instead of K_2CO_3	23/–
9	NaOAc instead of K_2CO_3	31/–
10	Cs_2CO_3 instead of K_2CO_3	29/–
11	without $[Ru(p\text{-cymene})Cl_2]_2$	n.d/–
12	without $AgNTf_2$	31/–
13	without K_2CO_3	n.d/–
14	without Ag_2O	13/–
15	none	67/21
16	without K_2CO_3	n.d/0
17	without $AgNTf_2$	11/0
18	without $[Ru(p\text{-cymene})Cl_2]_2$	n.d/0
19	CH_3CN instead of DCE	21/0
20	HFIP instead of DCE	51/21
21	toluene instead of DCE	23/0
22	1,4-dioxane instead of DCE	51/25
23	K_3PO_4 instead of K_2CO_3	36/5
24	NaOAc instead of K_2CO_3	41/7
25	Na_2CO_3 instead of K_2CO_3	33/21
26	3.0 equiv. K_2CO_3 for 36 h	16/73

[a]Reaction conditions for **3aa**: **1a** (0.20 mmol), **2a** or **2a'** (entries 1–25, 0.30 mmol), $[Ru(p\text{-cymene})Cl_2]_2$ (10 mol%), $AgNTf_2$ (40 mol%), Ag_2O (entries 1–14, 2 equiv.), K_2CO_3 (2 equiv.) in DCE (1.5 mL) at 120 °C for 16 h. [a]Reaction conditions for **4aa**: **1a** (0.20 mmol), **2a'** (entry 26, 0.44 mmol), $[Ru(p\text{-cymene})Cl_2]_2$ (10 mol%), $AgNTf_2$ (40 mol%), K_2CO_3 (3 equiv.) in DCE (1.5 mL) at 120 °C for 36 h. [b]Isolated yield.

The optimization of the alkynylation of (1-methyl-1*H*-imidazol-2-yl)benzophenone **1a** was investigated using either TIPS-protected terminal alkyne **2a** or TIPS-protected bromoalkyne **2a'** as the alkynyl source (Table 1). We initially focused on oxidative *ortho* alkynylation. Employing 10 mol% $[Ru(p\text{-cymene})Cl_2]_2$ as the catalyst in DCE, along with $AgNTf_2$ (40 mol%), Ag_2O (2 equiv.), and K_2CO_3 (2 equiv.), afforded the desired alkynylation product **3aa** in 73% yield (entry 1). However, replacing DCE with acetonitrile, toluene, or 1,4-dioxane resulted in lower yields (entries 2–4). We then screened various additives, including AgOAc, Ag_2CO_3, $Cu(OAc)_2$, K_3PO_4, NaOAc, and Cs_2CO_3, but none provided improved results (entries 5–10). Control experiments confirmed that $[Ru(p\text{-cymene})Cl_2]_2$, $AgNTf_2$, Ag_2O, and K_2CO_3 were essential for the reaction (entries 11–14). Next, we optimized the reaction conditions for *ortho* alkynylation using **2a'** as the alkynyl source. To our delight, employing 10 mol% $[Ru(p\text{-cymene})Cl_2]_2$, along with $AgNTf_2$ (40 mol%) and K_2CO_3 (2 equiv.) in DCE, yielded the alkynylated product **3aa** in 67% yield with an acceptable selectivity (entry 15). Control experiments further confirmed that $[Ru(p\text{-cymene})Cl_2]_2$, $AgNTf_2$, and K_2CO_3 were indispensable (entries 16–18). Solvent screening revealed that alternative solvents resulted in diminished yields (entries 19–22), and testing different bases did not lead to improved outcomes (entries 23–25). Finally, we discovered that increasing K_2CO_3 to 3 equiv. and extending the reaction time to 36 h led to the formation of the dialkynylated product **4aa** in 73% yield (entries 26). Notably, these optimized reaction conditions are air-stable and can be conveniently carried out on the benchtop.

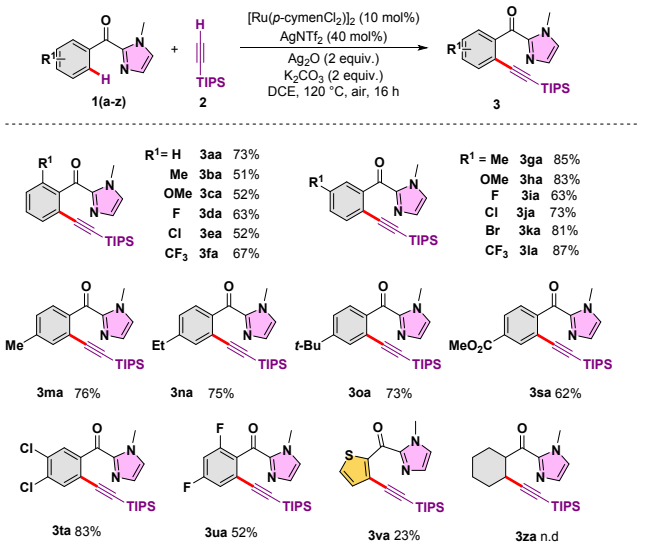

Scheme 2 Scope of oxidative *ortho*-alkynylation

Next, we explored the scope of the oxidative *ortho*-alkynylation reaction under standard conditions (Scheme 2). A variety of electron-withdrawing and electron-donating groups at the *ortho*, *meta*, and *para* positions were well tolerated, affording the desired alkynylation products (**3aa–3sa**) in yields ranging from 51% to 87%. Notably, substrates bearing double electron-withdrawing groups led to the target products (**3ta** and **3ua**) in good to excellent yields. Additionally, replacing the phenyl group with a thiophene ring was compatible with this strategy, yielding **3va** in 23% yield. However, cyclohexyl-substituted 2-acylimidazole failed to produce the expected product **3za**.

Encouraged by the preliminary results, we next explored the scope of *ortho*-monoalkynylation under the optimized

Journal Name ARTICLE

View Article Online
DOI: 10.1039/D5QO00868A

conditions (Scheme 3). A variety of substituents on the benzene ring, including methyl, ethyl, *tert*-butyl, methoxy, fluorine, chlorine, bromine, trifluoromethyl, and methyl carbonate, were well tolerated, affording the desired products (**3aa**–**3sa**) in yields ranging from 47% to 83%. Disubstituted substrates successfully generated **3ta** and **3ua** with yields of 76% and 52%, respectively. Interestingly, the substrate containing a thiophene ring produced the corresponding product **3va** in 32% yield. Unfortunately, the substrate **1z** failed to furnish the expected product **3za**.

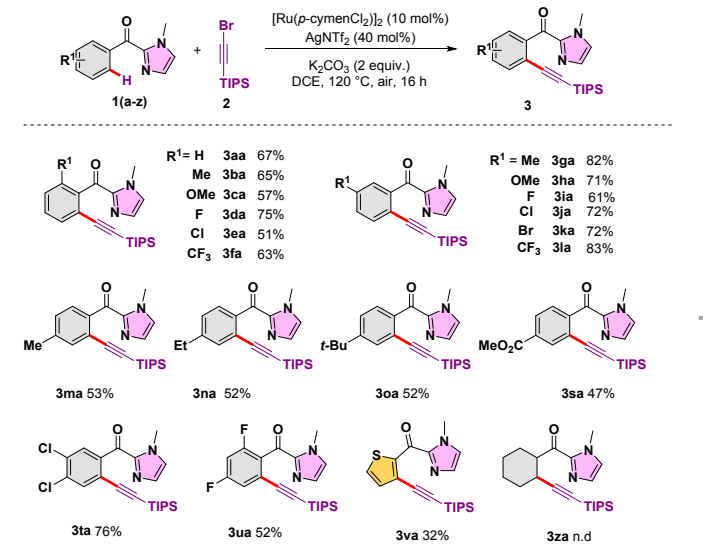

Scheme 3 Scope of *ortho*-monoalkynylation

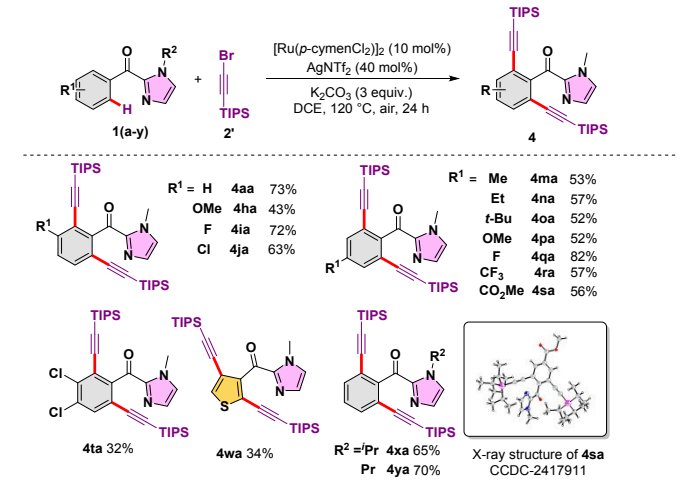

Scheme 4 Scope of *ortho*-dialkynylation

Furthermore, we evaluated the reaction scope for *ortho*-dialkynylation (Scheme 4). Various 2-acylimidazole derivatives substituted at the *meta* and *para* positions on the benzene ring were well tolerated, affording the desired products (**4aa**–**4sa**) in good to excellent yields. The structure of the product **4sa** was confirmed by X-ray diffraction analysis. Delightfully, the substrate **1t** could afford the corresponding product **4ta** in a relatively lower yield due to the steric hindrance. Encouragingly, the optimized reaction conditions were also effective for the formation of the thienyl product **4wa** in 34% yield. Additionally, different *N*-substituents were well tolerated, yielding **4xa** and **4ya** in 65% and 70%, respectively.

As the detailed mechanism remains to be elucidated, a series of preliminary mechanistic studies were conducted (Scheme 5). First, silver acetylide was successfully synthesized and subjected to oxidative *ortho*-alkynylation with Ag_2O or without Ag_2O under standard conditions, affording the desired product **3aa** in 65% and 60%, respectively (Scheme 5a). This result suggests that the reaction involves the formation of an alkynyl-Ag species, which may undergo transmetalation to generate a Ru-alkynyl intermediate. Next, the addition of the radical scavenger TEMPO had no effect on the *ortho*-alkynylation process, indicating that a radical pathway is not involved (Scheme 5b). Furthermore, H/D scrambling experiments conducted in the absence of compound **2a'** demonstrated the reversibility of C–H bond cleavage (Scheme 5c). Finally, the kinetic isotope effect (KIE) values of K_H/K_D were determined to be 3.76 for the oxidative *ortho*-alkynylation and 3.34 for the *ortho*-alkynylation (Scheme 5d). These results suggest that C–H bond cleavage is the rate-determining step in both reactions.

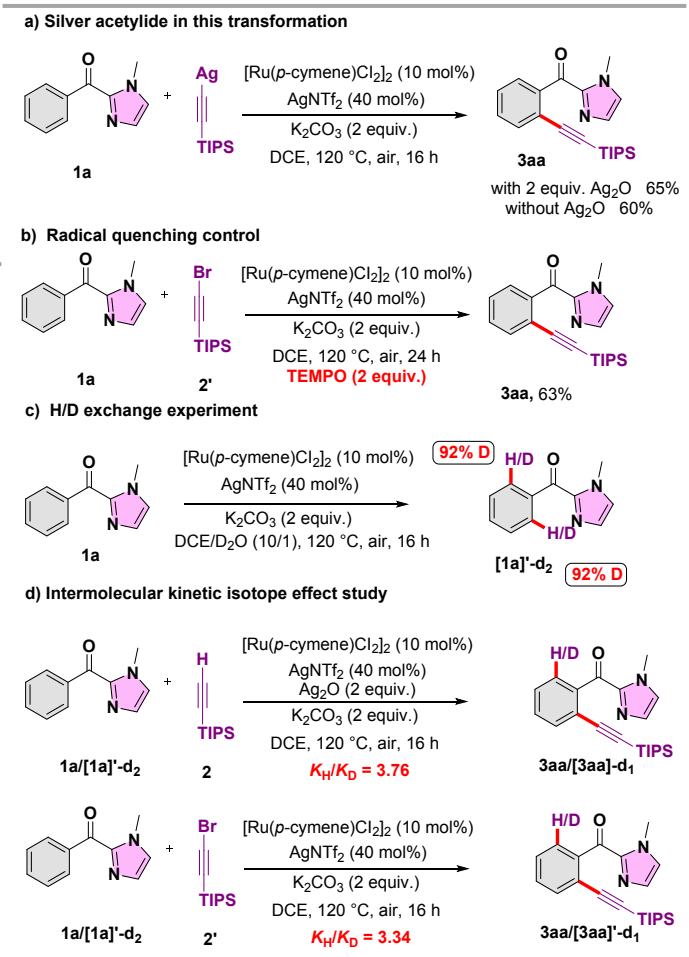

Scheme 5 Control experiments

Based on the aforementioned studies and previous research, we propose two possible catalytic mechanisms (Scheme 6). In the oxidative *ortho*-alkynylation using a TIPS-protected terminal alkyne **2a** as the alkynyl source,[15] the Ru(II) catalytic precursor is initially generated in the presence of $AgNTf_2$. This species

View Article Online
DOI: 10.1039/D5QO00868A

coordinates with substrate **1a** and undergoes base-assisted deprotonation at the *ortho*-C–H bond to form the ruthenacycle intermediate **I**. Intermediate **I** then undergoes transmetalation with the in situ generated alkynyl silver species to afford the alkynyl–ruthenium complex **II**. Subsequent reductive elimination furnishes the product **3aa** and a Ru(0) species, which is reoxidized by Ag_2O to regenerate the active Ru(II) catalyst. In the *ortho*-alkynylation using a TIPS-protected bromoalkyne **2a'** as the alkynyl source,[16] a similar six-membered ruthenacycle intermediate **I** is formed and coordinates with substrate **2a'**. This is followed by alkyne incorporation to generate intermediate **IV**, which undergoes base-assisted *β*-bromide elimination to deliver the product **3aa** and KBr, along with the regeneration of the active Ru(II) catalyst.

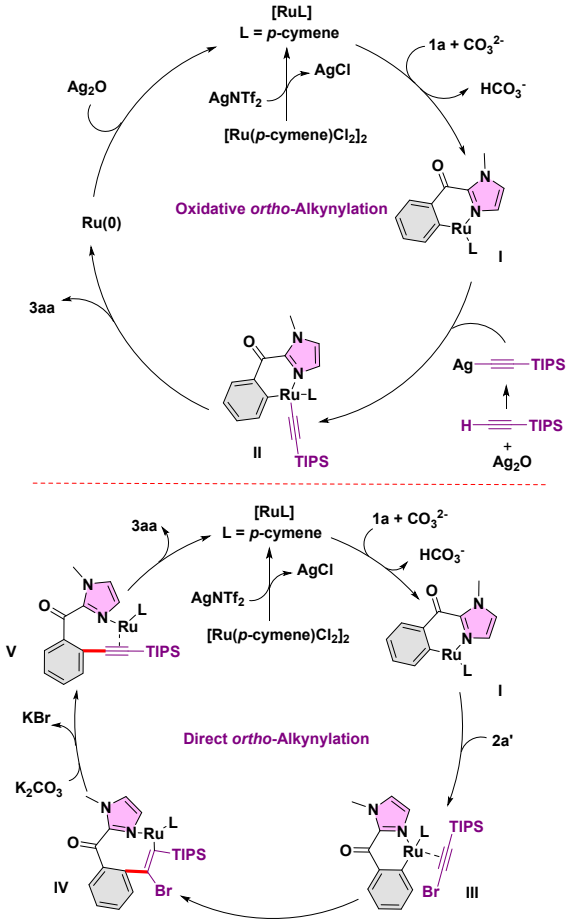

Scheme 6 Plausible reaction pathways

To evaluate the practical applicability of this strategy, gram-scale reactions and post-synthetic modifications were carried out (Scheme 7). The products **3aa** and **4aa** were obtained in 65% and 67% yields, respectively, on a 3.0 mmol scale. Subsequent deprotection of the TIPS group using TBAF afforded the terminal di-alkyne product **5** in 80% yield, representing a more synthetically valuable compound. Furthermore, the bromo-substituted product **3ka** underwent a Suzuki coupling reaction with phenylboronic acid to afford the corresponding product **6** in 85% yield. Notably, the imidazole group could be readily removed to generate ester **7**, which was further transformed into valuable derivatives **8** and **9**, demonstrating the broad synthetic utility of this protocol. Finally, under standard conditions with a TIPS-protected bromoalkyne as the alkynyl source, 2-acylimidazole derivatives containing drug-like molecular scaffolds were well tolerated, and the target products **10** and **11** were obtained in good yields.

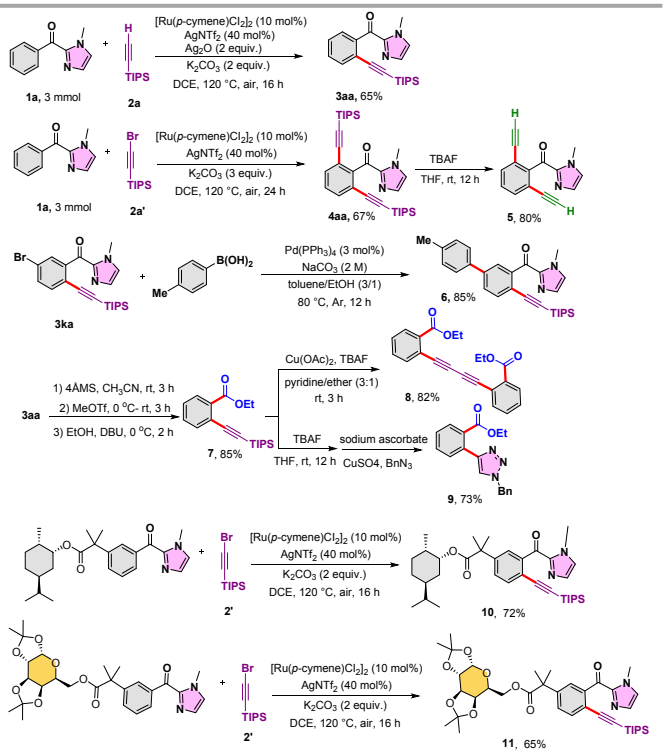

Scheme 7 Gram-scale synthesis and transformations

Conclusions

In summary, we have developed a Ru(II)-catalyzed *ortho*-alkynylation of 2-acylimidazole derivatives using either TIPS-protected terminal alkynes or TIPS-protected bromoalkynes. This protocol offers a valuable approach for the synthesis of diverse molecular building blocks and is particularly promising for late-stage functionalization, with potential applications in medicinal chemistry and materials science.

Author contributions

Y. Gui, X. Li and T. Fu performed the experiments, collected and analyzed the data. Y. Gui and X. Li wrote the original draft. T. Liang and Z. Li assisted in revising the manuscript. S. Zhao and Z. Zhang conceived and directed the project and revised the manuscript. All authors discussed the results and commented on the manuscript.

Data availability

The data supporting this article have been included as part of the ESI.†

Conflicts of interest

There are no conflicts to declare.

Acknowledgements

This work is supported by the National Natural Science Foundation of China (22461003), the Natural Science Foundation of Guangxi Province (2025GXNSFAA069547), Guangxi Major Talent Project, and the Opening Project of Guangxi Key Laboratory of Petrochemical Resource Processing and Process Intensification Technology (2023K017).

Notes and references

1 (a) Hofmann, K., *I*midazole and Its Derivatives, Volume 6, Part 1., *John Wiley & Sons,* 2009; (b) Olender, D., Zwawiak, J., Lukianchuk, V., Lesyk, R., Kropacz, A., Fojutowski, A. and Zaprutko, L., Synthesis of some *N*-substituted nitroimidazole derivatives as potential antioxidant and antifungal agents. *Eur. J. Med. Chem.*, 2009, **44**, 645−652; (c) Zhang, M., Hua, H., Dai, P., He, Z., Han, L., Tang, P., Yang, J., Lin, P., Zhang, Y., Zhan, D., Chen, J., Qiao, Y., Li, C. C., Zhao, J. and Yang, Y., Dynamically interfacial pH-buffering effect enabled by *N*-methylimidazole molecules as spontaneous proton pumps toward highly reversible Zinc-metal anodes. *Adv. Mater.*, 2023, **35**, e2208630; (d) Mota, F. A. S., Liu, M., Mohsen, A. A. A., Yao, X., Mai, Z. and Tang, C., Development of Polyamine/Alkanolamine-based Hypergolics with hydrogen Peroxide: A new route to *N*-methylimidazole with MDEA as a promising green fuel. *Fuel*, 2024, **357**, 129798.

2 (a) Gaba, M. and Mohan, C., Development of drugs based on imidazole and benzimidazole bioactive heterocycles: recent advances and future directions. *Med. Chem. Res.,* 2015, **25**, 173−210; (b) Fan, Y. L., Jin, X. H., Huang, Z. P., Yu, H. F., Zeng, Z. G., Gao, T. and Feng, L. S., Recent advances of imidazole-containing derivatives as anti-tubercular agents. *Eur. J. Med. Chem.*, 2018, **150**, 347−365.

3 (a) Li, S. W., Wan, Q. and Kang, Q., Chiral-at-Metal Rh(III) Complex-Catalyzed Michael Addition of Pyrazolones with *α,β*-Unsaturated 2-Acyl Imidazoles. *Org. Lett.*, 2018, **20**, 1312−1315; (b) Lu, R., Zhang, Q. and Guo, C., Catalytic stereodivergent allylic alkylation of 2-acylimidazoles for natural product synthesis. *Nat. Commun.* 2023, **14**, 8118.

4 (a) Huo, H., Shen, X., Wang, C., Zhang, L., Röse, P., Chen, L.-A., Harms, K., Marsch, M., Hilt, G. and Meggers, E., Asymmetric photoredox transition-metal catalysis activated by visible light. *Nature*, 2014, **515**, 100−103; (b) Lauberteaux, J., Pichon, D., Baslé, O., Mauduit, M., Marcia de Figueiredo, R. and Campagne, J. M., Acyl-Imidazoles: A Privileged Ester Surrogate for Enantioselective Synthesis. *ChemCatChem*, 2019, **11**, 5705−5722; (c) Kang, T., Hou, L., Ruan, S., Cao, W., Liu, X. and Feng, X., Lewis acid-catalyzed asymmetric reactions of *β,γ*-unsaturated 2-acyl imidazoles. *Nat. Commun.* 2020, **11**, 3869.

5 (a) Trost, B. M. and Li, C.-J., *Modern alkyne chemistry: Catalytic and atom-economic transformations*., *John Wiley & Sons*, 2015; (b) Trost, B. M. and Masters, J. T., Transition metal-catalyzed couplings of alkynes to 1,3-enynes: modern methods and synthetic applications. *Chem. Soc. Rev.*, 2016, **45**, 2212−2238; (c) Talele, T. T., Acetylene group, friend or foe in medicinal chemistry. *J. Med. Chem.*, 2020, **63**, 5625−5663; (d) He, B., Huang, J., Liu, X., Zhang, J., Lam, J. W. Y. and Tang, B. Z., Polymerizations of Activated Alkynes. *Prog. Polym. Sci.*, 2022, **126**, 101503; (e) Cao, Y., Fang, H., Guo, C., Sun, W., Xu, Y., Wu, Y. and Wang, Y., Alkynyl boosted high-performance lithium storage and mechanism in covalent phenanthroline framework. *Angew. Chem. Int. Ed.*, 2023, **62**, e202302143.

6 (a) Chinchilla, R. and Nájera, C., Recent advances in Sonogashira reactions. *Chem. Soc. Rev.*, 2011, **40**, 5084−5121; (b) He, C., Ke, J., Xu, H. and Lei, A., Synergistic catalysis in the sonogashira coupling reaction: quantitative kinetic investigation of transmetalation. *Angew. Chem. Int. Ed.*, 2013, **52**, 1527−1530; (c) Choy, P. Y., Gan, K. B. and Kwong, F. Y., Recent expedition in Pd-catalyzed sonogashira coupling and related processes *Chin. J. Chem.*, 2023, **41**, 1099−1118.

7 (a) Besselièvre, F. and Piguel, S., Copper as a Powerful Catalyst in the Direct Alkynylation of Azoles. *Angew. Chem. Int. Ed.*, 2009, **48**, 9553-9556; (b) Jiang, G., Hu, W., Li, J., Zhu, C., Wu, W. and Jiang, H., Palladium-catalyzed primary amine-directed regioselective mono- and di-alkynylation of biaryl-2-amines. *Chem. Commun.*, 2018, **54**, 1746−1749; (c) Tan, E., Zanini, M. and Echavarren, A. M., Iridium-Catalyzed *β*-Alkynylation of Aliphatic Oximes as Masked Carbonyl Compounds and Alcohols. *Angew. Chem. Int. Ed.* 2020, **59**, 10470−10473; (d) Suseelan Sarala, A., Bhowmick, S., de Carvalho, R. L., Al-Thabaiti, S. A., Mokhtar, M., da Silva Júnior, E. N. and Maiti, D., Transition-metal-catalyzed selective alkynylation of C–H bonds. *Adv. Synth. Catal.* 2021, **363**, 4994−5027.

8 Tobisu, M., Ano, Y. and Chatani, N., Palladium-Catalyzed Direct Alkynylation of C–H Bonds in Benzenes. *Org. Lett.*, 2009, **11**, 3250−3252.

9 Xie, F., Qi, Z., Yu, S. and Li, X., Rh(III)- and Ir(III)-catalyzed C–H alkynylation of arenes under ahelation assistance. *J. Am. Chem. Soc.*, 2014, **136**, 4780−4787.

10 (a) Ruan, Z., Sauermann, N., Manoni, E. and Ackermann, L., Manganese-catalyzed C–H alkynylation: expedient peptide synthesis and modification. *Angew. Chem. Int. Ed.*, 2017, **56**, 3172−3176; (b) Kaplaneris, N., Son, J., Mendive-Tapia, L., Kopp, A., Barth, N. D., Maksso, I., Vendrell, M. and Ackermann, L., Chemodivergent manganese-catalyzed C–H activation: modular synthesis of fluorogenic probes. *Nat. Commun.*, 2021, **12**, 3389.

11 Kuang, X., Li, J. J., Liu, T., Ding, C. H., Wu, K., Wang, P. and Yu, J. Q., Cu-mediated enantioselective C–H alkynylation of ferrocenes with chiral BINOL ligands. *Nat. Commun.*, 2023, **14**, 7698.

12 Ortiz, E., Evarts, M. M., Strong, Z. H., Shezaf, J. Z. and Krische, M. J., Ruthenium-catalyzed C–C Coupling of terminal alkynes with primary alcohols or aldehydes: *α,β*-acetylenic ketones (ynones) *via* oxidative alkynylation. *Angew. Chem. Int. Ed.*, 2023, **62**, e202303345.

13 (a) Huo, H., Wang, C., Harms, K. and Meggers, E., Enantioselective, catalytic trichloromethylation through visible-light-activated photoredox catalysis with a chiral Iridium complex. *J. Am. Chem. Soc.*, 2015, **137**, 9551−9554; (b) Zhou, Z., Li, Y., Han, B., Gong, L. and Meggers, E., Enantioselective catalytic *β*-amination through proton-coupled electron transfer followed by stereocontrolled radical-radical coupling. *Chem. Sci.*, 2017, **8**, 5757−5763; (c) Fan, L. F., Luo, S. W., Chen, S. S., Wang, T. C., Wang, P. S. and Gong, L. Z., Nucleophile Coordination Enabled Regioselectivity in Palladium-Catalyzed Asymmetric Allylic C–H Alkylation. *Angew. Chem. Int. Ed.*, 2019, **58**, 16806−16810; (d) Wang, T. C., Fan, L. F., Shen, Y., Wang, P. S. and Gong, L. Z., Asymmetric allylic C–H alkylation of allyl ethers with 2-acylimidazoles. *J. Am. Chem. Soc.*, 2019, **141**, 10616−10620; (e) Xu, N., Pu, M., Yu, H., Yang, G., Liu, X. and Feng, X., Iron-Catalyzed Asymmetric *α*-Alkylation of 2-Acylimidazoles *via* Dehydrogenative Radical Cross-Coupling with Alkanes. *Angew. Chem. Int. Ed.*, 2024, **63**, e202314256.

14 Mahato, S. K. and Chatani, N., The Iridium(III)-Catalyzed Direct C(sp^2)– and C(sp^3)–H Alkynylation of 2-Acylimidazoles with

View Article Online
DOI: 10.1039/D5QO00868A

Various Alkynyl Bromides: Understanding the Full Catalytic Cycle. *ACS Catal.*, 2020, **10**, 5173−5178.

15 (a) Kim, S. H., Park, S. H. and Chang, S., Palladium-catalyzed oxidative alkynylation of arene C–H bond using the chelation-assisted strategy. *Tetrahedron*, 2012, **68**, 5162−5166; (b) Zhou, J., Shi, J., Qi, Z., Li, X., Xu, H. E. and Yi, W., Mild and Efficient Ir(III)-Catalyzed Direct C–H Alkynylation of *N*-Phenoxyacetamides with Terminal Alkyne. *ACS Catal.*, 2015, **5**, 6999−7003; (c) Wu, G., Ouyang, W., Chen, Q., Huo, Y. and Li, X., Cross-dehydrogenative alkynylation of sulfonamides and amides with terminal alkynes *via* Ir(III) catalysis. *Org. Chem. Front.*, 2019, **6**, 284−289.

16 (a) Tan, E., Quinonero, O., Elena de Orbe, M. and Echavarren, A. M., Broad-Scope Rh-Catalyzed Inverse-Sonogashira Reaction Directed by Weakly Coordinating Groups. *ACS Catal.*, 2018, **8**, 2166−2172; (b) Tan, E., Nannini, L. J., Stoica, O. and Echavarren, A. M., Rh-catalyzed *ortho* C–H alkynylation of aromatic aldehydes. *Org. Lett.*, 2021, **23**, 1263−1268; (c) Niu, R. H., Zhang, J., Zhao, R. Y., Luo, Q. J., Li, J. H. and Sun, B., Cobalt(III)-catalyzed directed C-7 selective C–H alkynylation of indolines with bromoalkynes. *Org. Lett.*, 2023, **25**, 5411−5415.

View Article Online
DOI: 10.1039/D5QO00868A

Data Availability Statement

The data underlying this study are available in the published article and its ESI. The Supporting Information is available free of charge on the RSC Publications website at DOI:
Detailed experimental procedures, characterization data, crystallographic data for **4sa** (CIF), copies of NMR spectra for all isolated compounds.